Effect of Stator Slotting in the Magnetic Field Distribution of Linear Brushless Permanent Magnet Motor

Myung-Jin Chung, M. G. Lee, S. Q. Lee and Dae-Gab Gweon

Department of Mechanical Engineering, Korea Advanced Institute of Science and Technology,
373-1, Kusung-Dong, Yusong-Gu, Taejon 305-701, Korea

A model to describe the effect of stator slotting in the airgap region of a linear brushless permanent magnet motor (LBLPMM) is proposed for analytical prediction of magnetic field distribution. It is a two-dimensional model based on superposition of the effect of stator slotting and main field due to permanent magnet (PM) without stator slotting. The effect of stator slotting is expressed in form of a generalized equation, which is obtained by numerical analysis and is a function of motor geometric parameters, so the proposed model effectively accounts for the effect of stator slotting in the airgap field distribution according to change of motor geometry or relative motion of stator and armature. Results of prediction from the proposed model are compared with corresponding finite element analysis.

Key words : effect of stator slotting, magnetic field distribution, superposition, motor

1. Introduction

In recent years, there has been a significant development of LBLPMM's according to requirement for controlling linear motion over several tens nanometer to hundreds of millimeter strokes in the semiconductor industries, precision manufacturing and so on. The principles of operation of these linear motors are similar to those of conventional DC or synchronous motors. Generally, in linear motors, the magnets are located on the stator and a three phase winding is located on the armature.

Accurate knowledge of the magnetic field distribution in the airgap region of LBLPMM is essential for the prediction of motor performance, such as acoustic noise and vibration spectra [1], cogging force distribution [2], and steady state and transient dynamic characteristics [3].

Many researchers have studied analytical methods for calculation of magnetic field distribution. Gu and Gao used the method of separation of variables to analyze the airgap field of a multi pole PM motor [4]. Boules predicted the field distribution by summation of the field generated by equivalent current carrying coils [5]. By this method, field focusing effect in the magnets and magnetization direction could be accounted in field analysis. By Zhu *et al.*, a more general solution of the field in polar coordinates has been generated in both internal and external rotor topology [6]. A method for modeling of the slot effect was also developed by uti-

lizing the concepts of permeance and magneto-motive-force on the magnet field distribution [7].

However, the prior analytical methods have not effectively accounted for the slot effect on airgap field distribution, which is critical for prediction of the PM motor performance. Also numerical methods, such as finite element method, can provide more accurate method in accounting of slot effect, but they are usually time consuming and difficult to apply to iterative design procedure such as optimization process compared with analytical method.

Therefore, in this paper, a model to describe the effect of stator slotting in the airgap region of LBLPMM is proposed for analytical prediction of the magnetic field distribution. The field distribution is obtained from the superposition of the effect of stator slotting and the main field due to PM without stator slotting. The effect of stator slotting is expressed in the form of a generalized equation, which is obtained by numerical analysis and is a function of motor geometric parameters. The results of prediction from the proposed model are compared with corresponding finite element analysis.

2. Calculation Method

The field distribution in the LBLPMM with stator slotting, whose geometrical structure is shown in Fig. 1, is obtained from the superposition of the effect of stator slotting and the main field due to PM, when stator slotting is

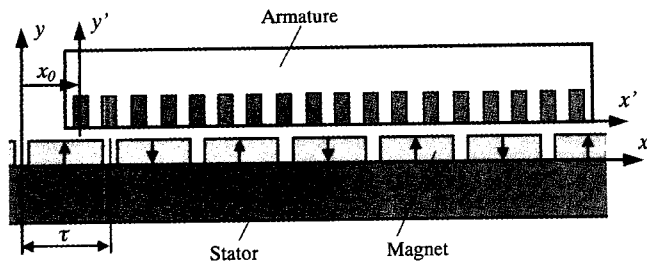*Tel: +82-42-869-3225,   e-mail: dggweon@cais.kaist.ac.kr

Fig. 1. Geometrical structure of LBLPMM.

Fig. 3. Analytical model of LBLPMM.

neglected, as in Fig. 2, and is expressed as follows

$$B_S(x, \ x_0) = B_M(x) + B_M(x) * \beta_{GES}(x, \ x_0) \qquad (1)$$

where $B_M(x)$ is the main field due to PM without stator slotting and is obtained by solving the governing two-dimensional Laplace's and Poisson's equations; $\beta_{GES}(x, x_0)$ is the generalized compensation factor by effect of stator slotting and is obtained by numerical analysis and is a function of the motor geometric parameters. x is a displacement from reference position at the stator with magnets and x_0 is a relative displacement from reference position of stator and armature.

3. Magnetic Field Produced by Permanent Magnet

The magnetic field analysis is performed for the analytical model of the LBLPMM shown in Fig. 3, where the stator slotting is neglected. In order to simplify the field calculation, the following assumptions are made:

· End effects are ignored.
· Permeability of iron parts in the armature and stator is infinite.
· Conductivities of all regions of the model are equal to zero.
· Permanent magnet has isotropic permeability, y-directed magnetization, and linear demagnetization characteristics.
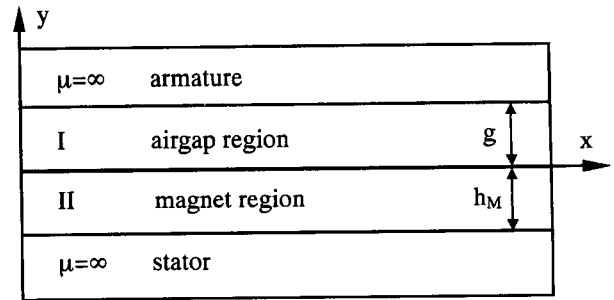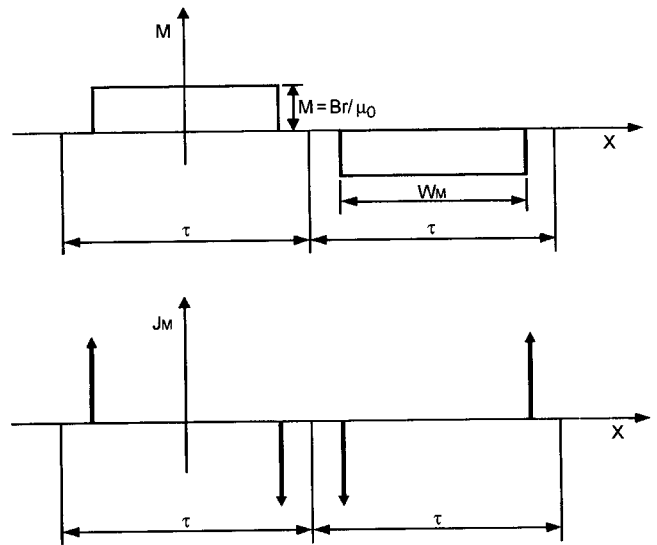

Fig. 4. Magnetization (M) and its equivalent magnetization current (J_M) of PM used in FEM.

3.1. Permanent Magnet Modeling

In Fig. 3, the PM is replaced by a continuous and isotropic region having the same permeability as the magnet recoil permeability μ_M. For the PM having a linear second-quadrant demagnetization characteristic, magnetization distribution is shown in Fig. 4 [6]. In form of Fourier series, the magnetization distribution is given by
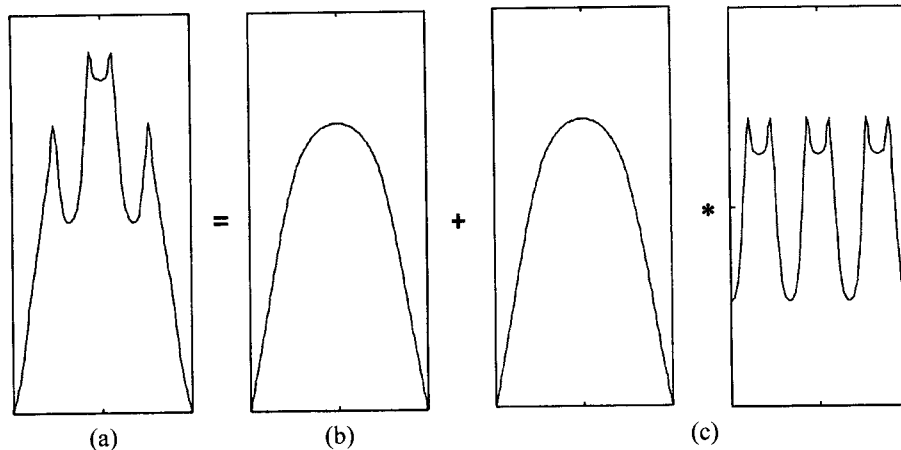

Fig. 2. Field distribution: (a) with stator slotting (b) without stator slotting (c) by compensation factor by effect of stator slotting.

$$M(x) = \sum_{n=1,3,5,\ldots}^{\infty} \frac{4}{n\pi}\frac{B_r}{\mu_0}\sin\frac{\alpha n\pi}{2}\cos\frac{n\pi x}{\tau} \tag{2}$$

where μ_0 is free space recoil permeability, τ is pole pitch, B_r is remanent magnetic field density, and α is ratio of width of magnet to the pole pitch.

The PM is modeled as equivalent magnetization current, which generates magnetic field equivalent to PM and the current is given by curl of magnetization as follows

$$J_M(x) = \nabla \times M$$

$$= -\sum_{n=1,3,5,\ldots}^{\infty} \frac{4B_r}{\tau\mu_0}\sin\frac{\alpha n\pi}{2}\sin\frac{n\pi x}{\tau} \tag{3}$$

where magnetization has y-directional component and equivalent magnetization current has z-directional component.

3.2. Magnetic Field Distribution

The partial differential equation for quasi-stationary magnetic fields in a continuous and isotropic region, as in Fig. 3, can be expressed in terms of magnetic vector potential A. For a two-dimensional problem the magnetic vector potential has only one component in the z-direction. For the airgap region I, Laplace's equation is

$$\frac{\partial^2 A_I}{\partial x^2} + \frac{\partial^2 A_I}{\partial y^2} = 0 \tag{4}$$

For the magnet region II, Poisson's equation is

$$\frac{\partial^2 A_{II}}{\partial x^2} + \frac{\partial^2 A_{II}}{\partial y^2} = -\mu_M J_M \tag{5}$$

where A_I and A_{II} are the z-directional magnetic vector potentials of each region.

The corresponding general solutions of (4) and (5) are given by

$$A_I(x,y) = \sum_{n=1,3,5,\ldots}^{\infty} \left(C_1 e^{\frac{n\pi x}{\tau}} + C_2 e^{-\frac{n\pi x}{\tau}} \right)\sin\frac{n\pi x}{\tau} \tag{6}$$

$$A_{II}(x,y) = \sum_{n=1,3,5,\ldots}^{\infty}$$
$$\left(C_3 e^{\frac{n\pi y}{\tau}} + C_4 e^{-\frac{n\pi y}{\tau}} + \frac{4B_r\tau}{n^2\pi^2}\sin\frac{\alpha n\pi}{2} \right)\sin\frac{n\pi x}{\tau} \tag{7}$$

From the assumption that permeability of armature and stator is infinite, and the boundary conditions at the interface between the different regions, the four unknown constants can be determined.

$$\frac{1}{\mu_0}\left(\frac{\partial A_I}{\partial y}\right)_{y=\delta} = 0$$

$$\frac{1}{\mu_M}\left(\frac{\partial A_{II}}{\partial y}\right)_{y=0} = \frac{1}{\mu_0}\left(\frac{\partial A_I}{\partial y}\right)_{y=0}, \quad \left(\frac{\partial A_{II}}{\partial x}\right)_{y=0} = \left(\frac{\partial A_I}{\partial x}\right)_{y=0}$$

$$\frac{1}{\mu_M}\left(\frac{\partial A_{II}}{\partial y}\right)_{y=-h_M} = 0$$

where δ is airgap length and h_M is magnet height.

The constants in (6) and (7) are as follows

$$C_1 = C_2 e^{\frac{-2n\pi\delta}{\tau}}$$

$$C_2 = \frac{\frac{4B_r\tau}{n^2\pi^2}\sin\frac{\alpha n\pi}{2}}{\left(e^{\frac{-2n\pi\delta}{\tau}}+1\right)+\dfrac{\mu_M\left(-e^{\frac{-2n\pi\delta}{\tau}}+1\right)\left(e^{\frac{2n\pi h_M}{\tau}}+1\right)}{\mu_0\left(e^{\frac{2n\pi h_M}{\tau}}-1\right)}}$$

$$C_3 = C_4 e^{\frac{2n\pi h_M}{\tau}}$$

$$C_4 = -\frac{\mu_M\left(-e^{\frac{-2n\pi\delta}{\tau}}+1\right)}{\mu_0\left(e^{\frac{2n\pi h_M}{\tau}}-1\right)}C_2$$

The constants are functions of the motor geometric parameters, δ, α, h_M, and the magnet properties, μ_M, B_r.

By curl of magnetic vector potential, the field distribution is

$$B_{Mx}\vec{i} + B_{My}\vec{j} = \frac{\partial A}{\partial y}\vec{i} - \frac{\partial A}{\partial x}\vec{j} \tag{8}$$

In (8), since the field on the interface of airgap to armature, $y=\delta$, has only the y-direction component, it is given by

$$B_M(x) = -\sum_{n=1,3,5,\ldots}^{\infty}$$

$$\frac{\frac{8B_r}{n\pi}\sin\frac{\alpha n\pi}{2}}{\left(e^{\frac{-2n\pi\delta}{\tau}}+1\right)+\dfrac{\mu_M\left(-e^{\frac{-2n\pi\delta}{\tau}}+1\right)\left(e^{\frac{2n\pi h_M}{\tau}}+1\right)}{\mu_0\left(e^{\frac{2n\pi h_M}{\tau}}-1\right)}}e^{-\frac{n\pi\delta}{\tau}}\cos\frac{n\pi x}{\tau} \tag{9}$$

3.3. Comparison with Finite Element Calculation

The geometric parameters of the prototype LBLPMM, which have been used in the FEM and analytical method for field calculation, are given in Table 1. The magnetization curve used in the FEM is shown in Fig. 4 and equiv-

Table 1. Geometric parameters of LBLPMM

Parameter	Symbol	Value	[Unit]
Slot pitch	τ_S	8	mm
Slot width	ω_s	4	mm
Slot depth	l_d	4	mm
Airgap length	δ	4	mm
Pole pitch	τ	24	mm
Magnet width	ω_M	17.5	mm
Magnet thickness	h_M	3	mm
Magnet remanence	B_r	1.17	T
Magnet recoil permeability	μ_M	$1.1\mu_0$	–
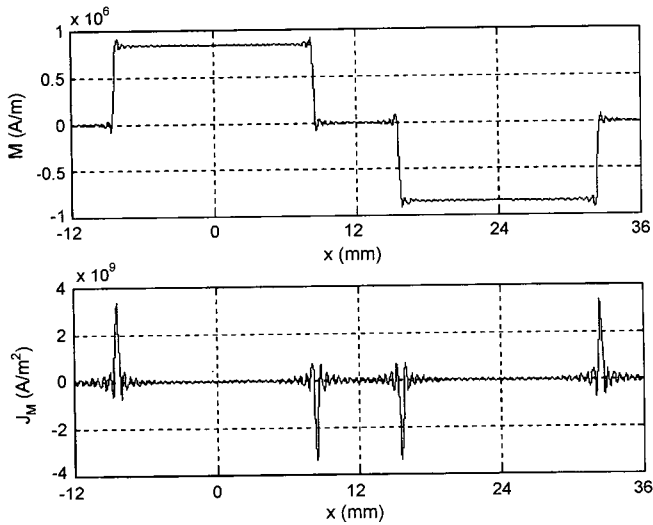
Fig. 5. Magnetization (M) and its equivalent magnetization current (J_M) of PM used in analytical calculation with 97th term by ignoring the higher order of Fourier series.
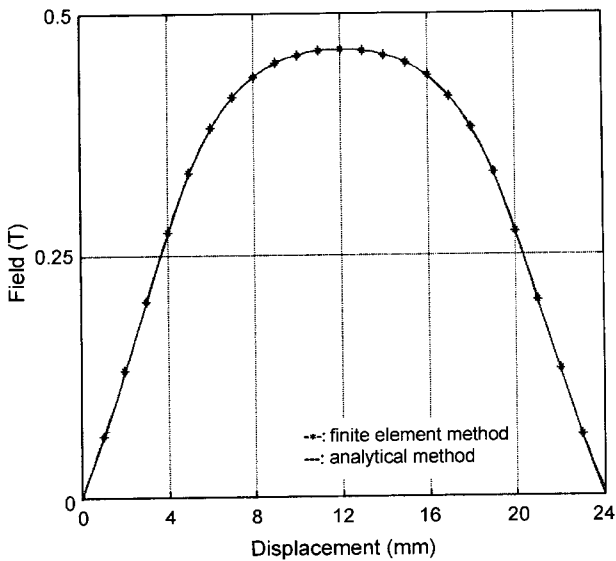

Fig. 6. Comparison of field distribution, $B_M(x)$, produced by PM at the airgap of LBLPMM without stator slotting.

alent magnetization current used in analytical calculation is shown in Fig. 5. The equivalent magnetization current is
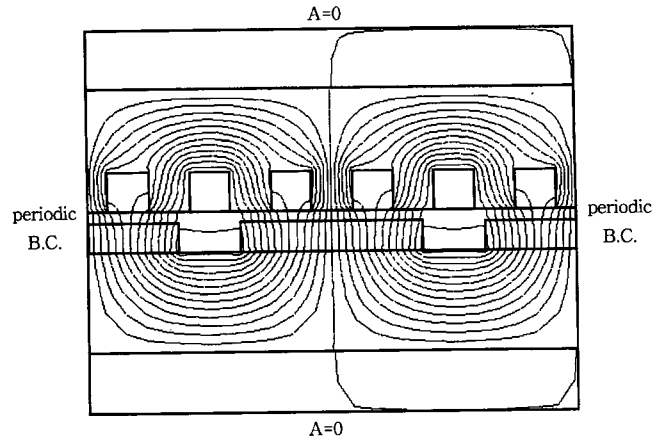

Fig. 7. Boundary conditions and field distribution of the analysis model.

different from delta-function at Fig. 4, because it is calculated from (3) with 97th term by ignoring the higher order of Fourier series. As shown in Fig. 6, the results obtained by the analytical calculation are in close agreement with those from the FEM for one pole pitch, because the effect of higher order terms ignored in analytical calculation is relatively small.

4. Modeling the Effect of Stator Slotting

From Fig. 2, a generalized compensation factor by effect of stator slotting, $\beta_{GES}(x, x_0)$, can be obtained from (1), if we can obtain magnetic field, $B_S(x, x_0)$, via finite element analysis for LBLPMM with stator slotting as Fig. 7. The effect of stator slotting is expressed in the form of generalized equation, which is a function of motor geometric parameters. This generalized equation can be used in various LBLPMMs, which have different geometries.

4.1. Analysis of Field Distribution

To describe the effect of stator slotting, we obtain $B_S(x,x_0)$ by using finite element analysis for LBLPMM with stator slotting. And $B_M(x)$ is obtained by solving the governing two-dimensional Laplace's and Poisson's equations when the slot is neglected. In calculation of the $B_M(x)$, Carter's coefficient (k_c) is used to get effective airgap length (δ_e), which is expressed as $\delta \cdot k_c$ [8]. The analysis is performed according to change of normalized motor geometric parameters such as airgap length, magnet thickness, slot depth and magnet width as listed in Table 2. In this analysis, we con-

Table 2. Normalized value of geometric parameters

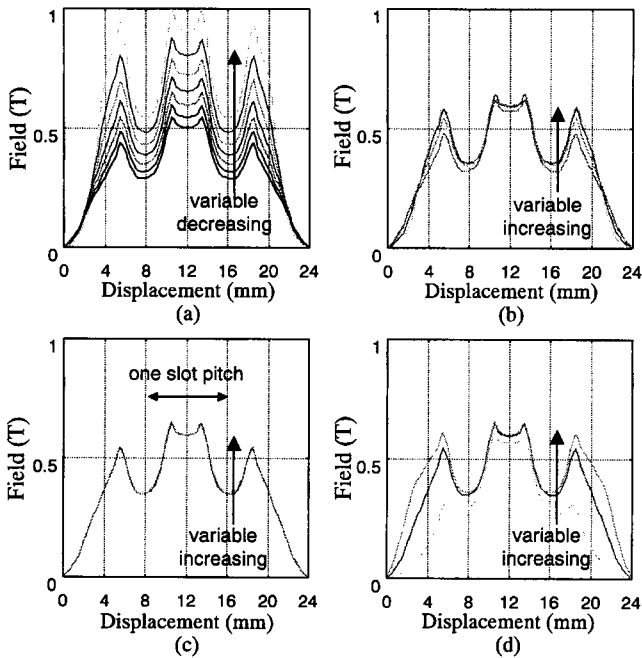| Parameter	Normalized value
Airgap length	0.3 0.5 0.68 0.8 1 1.2 1.5
Magnet thickness	0.06 0.1 0.15 0.19
Slot depth	0.08 0.16 0.25
Magnet width	0.5 0.8 0.9
where bold characters are nominal values	

Fig. 8. $B_S(x, x_0)$ obtained by finite element analysis when $x_0=0$ and stator slotting considered with respect to; (a) airgap length variation, (b) magnet thickness variation, (c) slot depth variation, (d) magnet width variation.
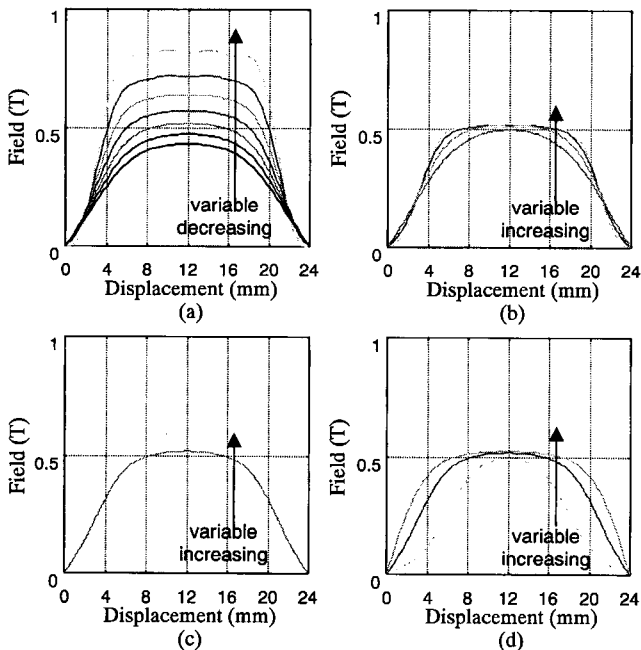

Fig. 9. $B_M(x)$ calculated by solving the governing two-dimensional Laplace's and Poisson's equation when stator slotting neglected with respect to; (a) airgap length variation, (b) magnet thickness variation, (c) slot depth variation, (d) magnet width variation.

sider the normal component of the field, because the component is used for motor performance calculation.

Fig. 8 and Fig. 9 show the normal component of the field on the interface of an airgap and armature obtained by finite element analysis and two-dimensional Laplace's and Pois-
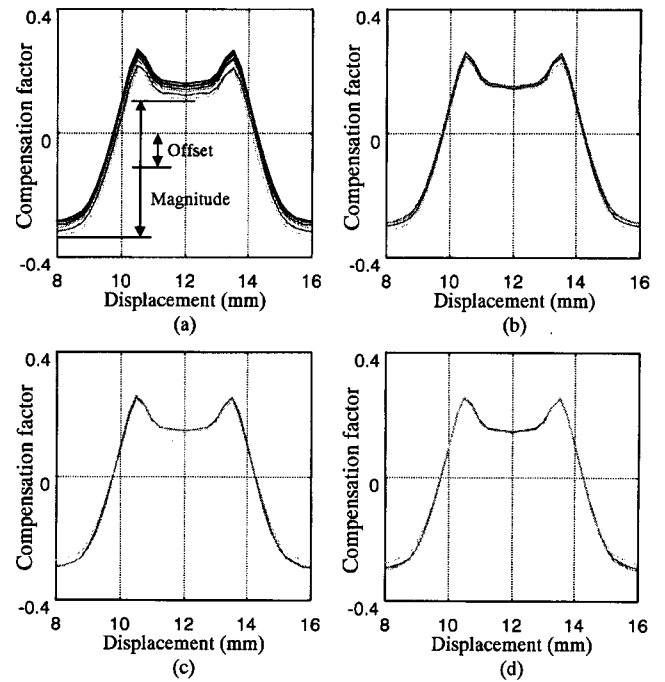

Fig. 10. $\beta_{GES}(x, x_0)$ by effect of stator slotting for one slot pitch with respect to; (a) airgap length variation, (b) magnet thickness variation, (c) slot depth variation, (d) magnet width variation when $x_0=0$.

son's equation, for one pole pitch repeated infinitely.

4.2. Modeling the Effect of Stator Slotting

Each generalized compensation factor accounting stator slotting for one slot pitch is obtained as in (10) for considered geometric parameters, and is shown in Fig. 10.

$$\beta_{GES}(x, x_0) = \frac{B_S(x, x_0) - B_M(x)}{B_M(x)} \qquad (10)$$

From Fig. 10, we know that the effect of stator slotting is similar to various geometric parameter values, except for airgap length. In Fig. 10(a), the characteristics of generalized compensation factor are magnitude and offset, where magnitude is difference between value at the center of tooth and value at the center of slot, and offset is the average value of the generalized compensation factor. The magni-

Table 3. Magnitude and offset value for airgap length variation

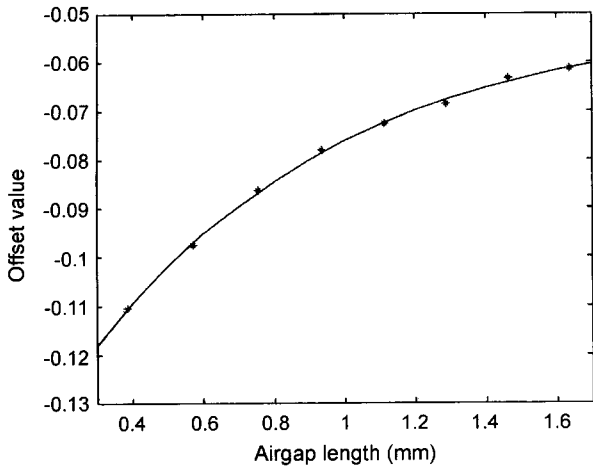| Airgap length	Characteristics	
	Magnitude	Offset
0.39	0.4413	−0.1104
0.57	0.4383	−0.0977
0.75	0.4381	−0.0863
0.93	0.4386	−0.0781
1.11	0.4384	−0.0727
1.29	0.4398	−0.0686
1.46	0.4413	−0.0632

Fig. 11. Curvefitted offset value according to airgap length: curvefitted coefficients are $a_0=-0.0545$, $a_1=-0.0974$, and $a_2=0.0384$.
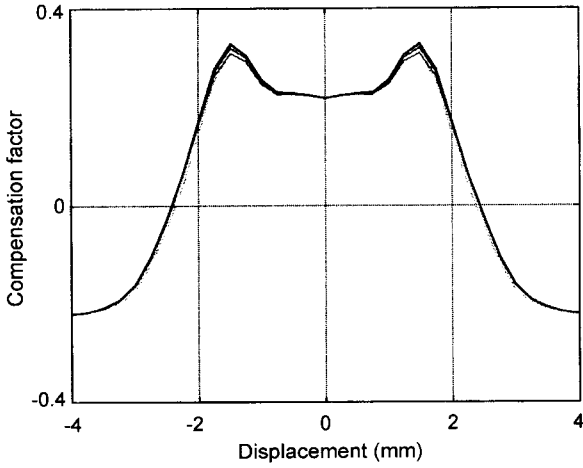

Fig. 12. Normalized field by effect of stator slotting when offset eliminated.

tude and offset value for the airgap length variation is shown in Table 3.

In Table 3, the magnitude has little variation, but the offset has uniform trend for airgap length variation. The offset value is curvefitted by Linear in the Parameters Regression method. The exponential function used in curvefitting is

$$\beta_{off}(\delta_n) = a_0 + a_1 e^{-\delta_n} + a_2 \delta_n e^{-\delta_n} \tag{11}$$

where β_{off} is the offset value, δ_n is the airgap length, and a_0, a_1, a_2 are coefficients to be curvefitted, and fitted data is shown in Fig. 11.

For airgap length variation, the generalized compensation factor is subtracted by curvefitted offset value as shown in Fig. 12, and described by Fourier series as

$$\beta_{ES}(x') = a_0 + \sum_{k=1,2,3,\dots}^{N/2} \left\{ a_k \cos\left(\frac{2\pi k x'}{\tau}\right) + b_k \sin\frac{2\pi k x'}{\tau} \right\} \tag{12}$$
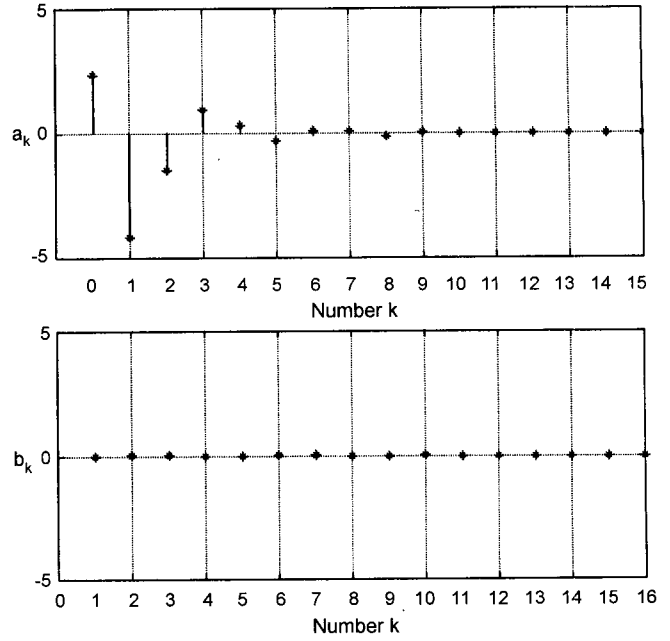

Fig. 13. The coefficients of Fourier series used in generalized compensation factor: (a) a_k for $k = 0, 1, 2, ..8$ and $a_k = 0$ for $k = 9, 10, .. 15$ (b) $b_k = 0$ for $k = 1, 2, .. 16$.

where $x'=x-x_0$, x' is a displacement from reference position at the armature. N is a number of data and a_0, a_k, and b_k are coefficients, and is shown in Fig. 13.

The generalized compensation factor by effect of stator slotting of (10) can be described as the summation of (11) and (12) as follows
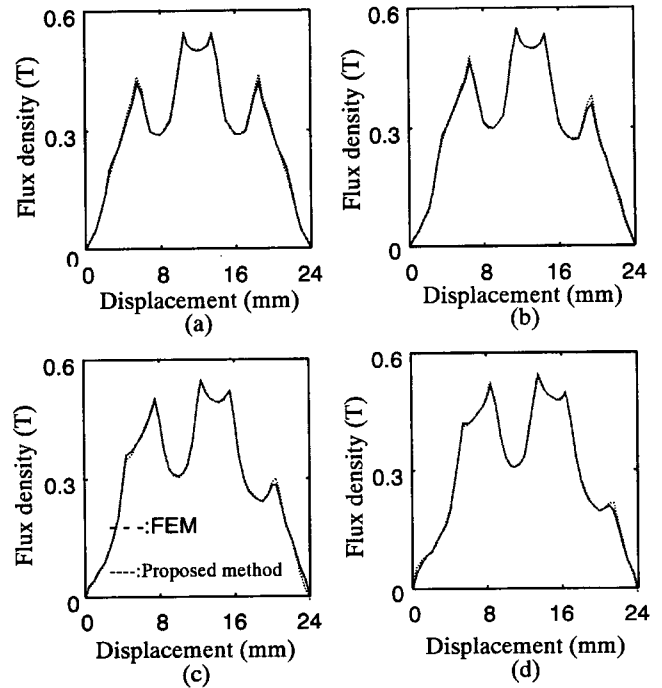

Fig. 14. Comparison of field distribution, $B_S(x, x_0)$, produced by PM in the 4 mm airgap of LBLPMM with stator slotting with respect to x_0 of stator and armature: (a) $x_0 = 0$ mm (b) $x_0 = 1$ mm (c) $x_0 = 2$ mm (d) $x_0 = 3$ mm.
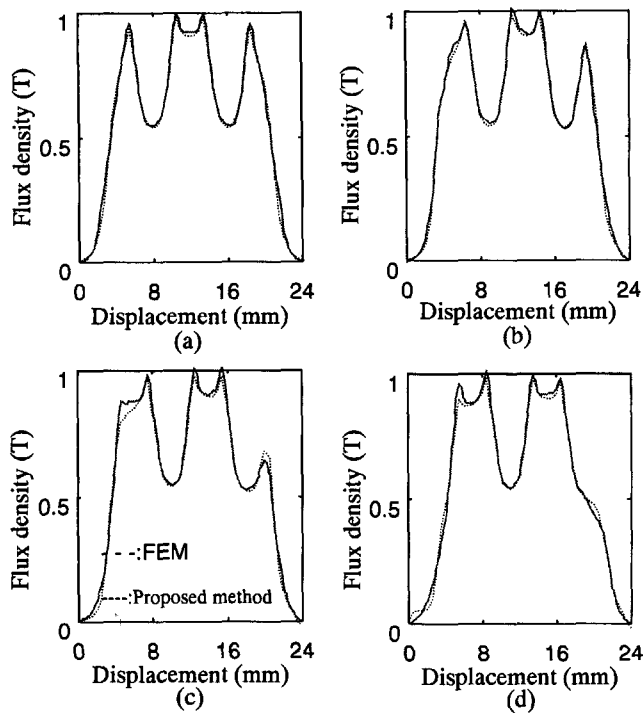
Fig. 15. Comparison of field distribution, $B_S(x, x_0)$, produced by PM in the 1 mm airgap of LBLPMM with stator slotting with respect to x_0 of stator and armature: (a) $x_0 = 0$ mm (b) $x_0 = 1$ mm (c) $x_0 = 2$ mm (d) $x_0 = 3$ mm.

$$\beta_{GES}(x, x_0) = \beta_{off}(\delta_n) + \beta_{ES}(x - x_0) \qquad (13)$$

When the airgap length of the LBLPMM is selected, (13) is determined. Using (9) and (13), we can analytically calculate magnetic field due to the PM in airgap for various geometric parameters of motor with stator slotting. Also, the effect of stator slotting on relative motion of stator and armature can be described by calculation of $\beta_{GES}(x, x_0)$ according to x_0.

4.3. Comparison with Finite Element Calculation

Field distribution obtained by using (9) and (13) is validated by comparing results from corresponding finite element calculations for prototype LBLPMM whose parameters are given in Table 1, and is shown in Fig. 14 and Fig. 15, for airgap of 4 mm and 1 mm, respectively and with respect to relative motion of stator and armature.

From Fig. 14 and Fig. 15, analytical prediction is very similar to results from the finite element calculation for

variation of motor geometry such as airgap length and relative motion of stator and armature. At the tooth tips, both results show the field increasing, which is due to field concentration and is not sufficiently described in other analytical methods. As shown in Fig. 14 and Fig. 15, proposed analytical method can account effectively for the effect of stator slotting on airgap field distribution such as field concentration.

5. Conclusion

A model to describe the effect of stator slotting in the airgap region of LBLPMM is proposed for analytical prediction of magnetic field distribution and is compared with finite element analysis. In this model, the field distribution includes the field by effect of stator slotting, such as field increasing at the tooth tips, which is not considered effectively in other analytical methods. The effect of stator slotting is expressed in the form of a generalized equation, which is function of motor geometric parameters. Therefore, this model can be considered as one of several analytical approaches to describe the effect of stator slotting in predicting magnetic field distribution in the airgap region of LBLPMM's. By using this proposed model, we can perform iterative work such as optimal design with quicker prediction of motor performances.

References

[1] B. Heller and V. Hamata, Harmonic Field Effects in Induction Machines. New York: Elsevier (1997).

[2] J. D. L. Ree and N. Boules, IEEE IAS Conf. Rec. 15-20 (1987).

[3] J. D. L. Ree and N. Boules, IEEE Trans. Energy Conversion 6, 155-161 (1991).

[4] Q. Gu and H. Gao, Electrical Machines and Power Systems 10, 459-470 (1985).

[5] N. Boules, IEEE Trans. on Industry Applications IA-21, 633-643 (1985).

[6] Z. Q. Zhu, D. Howe, E. Bolte and B. Ackermann, IEEE Trans. Magnetics 29(1), 136-143 (1993).

[7] Z. Q. Zhu and D. Howe, IEEE Trans. Magnetics 29(1), 144-152 (1993).

[8] D. C. Hanselman, Brushless Permanent-Magnet Motor Design, McGraw-Hill, New York (1994), pp. 22.